

# Phenologically explicit models for studying plant–pollinator interactions under climate change

William F. Fagan · Sharon Bewick · Steve Cantrell · Chris Cosner ·  
Isabela Galarda Varassin · David W. Inouye

Received: 1 November 2013 / Accepted: 30 January 2014 / Published online: 22 February 2014  
© Springer Science+Business Media Dordrecht 2014

**Abstract** Climate change is significantly influencing phenology. One potential effect is that historically interacting partners will respond to climate change at different rates, creating the potential for a phenological mismatch among previously synchronized interacting species, or even sexes of the same species. Focusing on plant demographics in a plant–pollinator interaction, we develop a hybrid dynamical model that uses a “non-autonomous” differential equation system (Zonneveld model) for within-season dynamics and discrete equations for season-to-season dynamics. Our model outlines how and when changes in the relative phenologies of an interacting species pair will alter the demographic outcome of the interaction. For our plant–pollinator system, we find that plant population growth rates are particularly sensitive to phenology mismatch when flowers are short-lived, when pollinators are short-lived, or when flowers and pollinators exhibit high levels of within-population synchrony in emergence or arrival dates. More generally, our aim is to introduce the use of hybrid dynamical models as a framework through which researchers

can directly explore the demographic consequences of climatically driven phenological change.

**Keywords** Allee effect · Flower senescence · Pollinator emigration · Non-autonomous ordinary differential equation · Temporal match-mismatch hypothesis · Phenology · Zonneveld equation

## Introduction

Climate change engenders a variety of phenological responses in natural systems, including changes in the timing of spring (Schwartz and Hanes 2010), changes in migration or the timing of migration relative to a required resource (McKinney et al. 2012; Zipkin et al. 2012), and changes in the timing of reproduction (Sheriff et al. 2011; Inouye 2008). Although there is a general trend toward earlier phenology (Parmesan 2007), shifts among interacting species may not be synchronous, or even concordant in the direction of change (Sherry et al. 2007; Visser and Both 2005; Edwards and Richardson 2004). As a result, species interactions can be disrupted (Forrest and Thomson 2011; Forrest et al. 2010; Visser and Holleman 2001; Visser et al. 1998). Several studies have used either long-term monitoring or short-term manipulation to examine relative phenology among interacting species. These studies suggest that partner species often show differential responses to the perturbation. For example, Visser and Holleman (2001) have observed greater advancement of winter moth (*Operophtera brumata*) phenology relative to budburst of their host plant the pedunculate oak (*Quercus robur*). Likewise, Doi et al. (2008) have reported earlier *Prunus* flowering, but no change in the appearance of an important butterfly pollinator, *Pieris rapae*. Finally, in the

---

**Electronic supplementary material** The online version of this article (doi:10.1007/s12080-014-0218-8) contains supplementary material, which is available to authorized users.

---

W. F. Fagan (✉) · S. Bewick · I. G. Varassin · D. W. Inouye  
Department of Biology, University of Maryland, College Park,  
MD 20742, USA  
e-mail: bfagan@umd.edu

S. Cantrell · C. Cosner  
Department of Mathematics, University of Miami, Coral Gables,  
FL 33124, USA

I. G. Varassin  
Department of Botany, Universidade Federal do Paraná, Curitiba,  
Paraná, Brazil

Rocky Mountains, the flowering phenology of early season plants has advanced relative to the hummingbirds that visit them and seems to be more sensitive to advancement of snowmelt than their syrphid fly pollinators (McKinney et al. 2012; Iler and Inouye 2013).

A number of studies have separately examined the demographic consequences of phenological mismatch. Many of these have used inference drawn from species occurrence patterns to conclude that phenological mismatch yields perturbations to survival and population abundance for at least one partner. As an example, earlier advancement of jumping plant lice (Psyllidae) relative to their willow host (*Salix lapponum*) is implicated in the low-elevation range boundary of plant lice (Hill and Hodkinson 1995). Similarly, delayed appearance of a lycaenid butterfly relative to its host plant has been attributed to poor survival in xerophytic regions (Rodríguez et al. 1994). There are, however, very few long-term field studies that investigate the impact of phenological change on interacting species (but see (Both et al. 2006) for an example of a system where one partner was tracked over 18 years). Instead, short-term manipulation experiments have served as a proxy. While these studies provide critical guidance about the consequences of temporal mismatch between species, conclusions are restricted to the immediate effects of phenological mismatch, such as increased pollination limitation (Rafferty and Ives 2011a, b), decreased food supply, altered competition (Rudolf and Singh 2013), or altered predation or survival over a single generation or life-stage (Russell and Louda 2004; Miller-Rushing et al. 2010). As a result, it is unclear what the demographic and ecological outcomes of modified species interactions will be.

To provide an integrative backdrop for the growing body of empirical research on phenological aspects of species interactions, we develop a modeling framework that outlines how and when changes in the relative phenologies of an interacting species pair will have demographic consequences. Previous models exploring the consequences of temporal mismatches in multispecies networks have often collapsed the issues of temporal overlap and variation in density into one of simple overlap using a phenological token approach (Encinas-Viso et al. 2012). However, when studying the dynamics among pairs or small sets of species, “phenologically explicit” models are possible, and can accommodate the clear, quantitative accounting of the interplay between density and timing as called for in Miller-Rushing et al. (2010).

Several phenologically explicit models exist (Miller-Rushing et al. 2010), and can be quite complex, even accounting for evolution (Johansson et al. 2012; Gilman et al. 2012). Recently, Nakazawa and Doi (2012) presented a simplified framework that focuses solely on population dynamics. They employed continuous time models in which phenology appears as time-varying coefficients and changes in phenology result in phase shifts in periodic terms. Like Nakazawa and

Doi, we focus on demographic models that ignore evolution. However, we suggest that, for many systems, the use of hybrid dynamical models is more appropriate than a continuous time framework. Hybrid dynamical models can better capture the discrete nature of seasonal reproduction that is typical of many pollinators in seasonal environments. They are also superior because biologically relevant phenology features (e.g., the widths of the plant and pollinator emergence windows) can be incorporated easily and transparently.

The approach that we present could be applied to any set of interacting species, for example competing species, antagonistic consumer–resource interactions, or parasitoid–host dynamics (e.g., scenarios in Nakazawa and Doi (2012)). However, for the sake of illustration, we focus on plant–pollinator interactions, because climate change is projected to affect these systems especially strongly (Memmott et al. 2007; Rafferty and Ives 2011a; McKinney et al. 2012). To simplify model interpretation, we only consider the demographics of one species, while keeping the demographics of the other species fixed. This is akin to considering a generalist–specialist pair where only the specialist population is sensitive to phenological mismatch, while the generalist can compensate by switching to another interaction partner. We will consider a specialist plant. A similar approach could be applied to scenarios with a specialist pollinator or to scenarios where both species are specialists, although the latter is unlikely (Bascompte et al. 2003).

In what follows, we show how a phenologically explicit hybrid dynamical model can be constructed for a plant–pollinator pair. The model that we develop is a detailed accounting of plant–pollinator interactions and includes terms for pollinator acquisition and loss of pollen, flower pollination, pollination limitation, flower senescence, and seed set. However, even in this rather complicated model, our hybrid dynamical approach makes inclusion of phenology straightforward. Once we have fully developed a phenologically explicit plant–pollinator model, we use it to explore the effects of plant–pollinator asynchrony on plant demographics. In particular, we focus on the phenological threshold separating an increasing plant population (growth rate  $>1$ ) from a decreasing plant population (growth rate  $<1$ ). First, we illustrate how this threshold is crossed with increasing phenological mismatch between the plant and pollinator populations. We then ask how the position of the threshold changes depending on system parameters. Specifically, we consider the level of asynchrony within the plant population, the level of asynchrony within the pollinator population, pollinator lifespan, flower lifespan, plant lifespan, and pollination rate. This allows us to identify contexts and species-pairs that are likely to be more or less sensitive to phenological mismatch. Ultimately, such information should help to guide plant–pollinator conservation strategies under anticipated climate change scenarios.

**Methods**

We assume a monoecious and potentially perennial plant and a generalist pollinator. Because the dynamics of a generalist are only weakly dependent on the availability of any one of its partners, we uncouple pollinator dynamics from plant dynamics by assuming that pollinator dynamics do not depend on the plant population. This simplifies model interpretation, but is not necessary for our modeling framework. To explore the consequences of phenological mismatch on the plant population, we develop a “non-autonomous” differential equation system for the within-season dynamics. Unlike many classical ecological models (logistic, Lotka-Volterra, MacArthur-Rosenzweig), a non-autonomous differential equation system allows the dynamics of the interacting species to depend explicitly on time via the time variable,  $t$ . Our approach builds on a class of non-autonomous differential equation models that have been used to study reproductive asynchrony and protandry in single populations or in two-sex populations (Calabrese et al. 2008; Larsen et al. 2013; Lynch et al. 2013). These models have been termed Zonneveld models in honor of the Dutch theoretician who explored them exten-

sively in the context of single population dynamics of butterflies (Zonneveld 1992; Zonneveld and Metz 1991), but they are equally applicable to other animals and plants.

Within-season dynamics

We express pollinator abundance ( $S$ ) as

$$\frac{dS}{dt} = \overbrace{S_0 g_s(t, \theta_s)}^{\text{arrival/emergence}} - \overbrace{\alpha_s S}^{\text{departure/death}} \tag{1}$$

where  $S_0$  is the total pollinator population size,  $g_s(t, \theta_s)$  is a probability density function that stipulates the rate at which pollinators arrive (e.g., as with migrating hummingbirds) or emerge (e.g., as with butterflies eclosing from pupae), and  $\alpha_s$  is a constant death rate (which can also be interpreted as a pollinator emigration rate). Distinguishing between pollinators with ( $R$ ) and without ( $Q$ ) pollen, the total pollinator population can be expressed as  $S=Q+R$ , while the abundance of each class changes according to the following dynamics

$$\frac{dQ}{dt} = \overbrace{S_0 g_s(t, \theta_s)}^{\text{arrival/emergence}} - \overbrace{\gamma(U + P)Q}^{\text{pollen collection}} - \overbrace{\alpha_s Q}^{\text{departure/death}} + \overbrace{\beta R}^{\text{pollen removal}} \tag{2}$$

$$\frac{dR}{dt} = \overbrace{\gamma(U + P)Q}^{\text{pollen collection}} - \overbrace{\alpha_s R}^{\text{departure/death}} - \overbrace{\beta R}^{\text{pollen removal}} \tag{3}$$

where  $U$  and  $P$  are the abundance of unpollinated and pollinated flowering plants, respectively,  $\gamma$  is the visitation rate of pollinators to flowering plants, and  $\beta$  is the rate at which pollen is removed from a pollinator (e.g., via grooming, brushing off on other plants, etc.). The structure of the pollen collection term assumes that pollinators can obtain pollen from both pollinated and unpollinated flowers, but this could be modified to allow for more complex scenarios in which pollinated flowers could have depleted pollen availability (e.g., orchid flowers, whose pollinia are removed by pollinators, or any flowers that shed pollen upon visitation) or in which pollination induces changes in flower structure that may dissuade pollinator visitation (Harder and Johnson 2005). The dynamics of the unpollinated and pollinated flowers are then described as

$$\frac{dU}{dt} = \overbrace{U_0 g_p(t, \theta_p)}^{\text{flower opening}} - \overbrace{\mu_p U}^{\text{flower death}} - \overbrace{\alpha_p n U}^{\text{plant death}} - \overbrace{\Lambda UR}^{\text{pollination}} \tag{4}$$

$$\frac{dP}{dt} = \overbrace{\Lambda UR}^{\text{pollination}} - \overbrace{\alpha_p n P}^{\text{plant death}} - \overbrace{\mu_p P}^{\text{flower death}} \tag{5}$$

where  $U_0$  is the total number of flowers in the system,  $g_p(t, \theta_p)$  is a probability density function that defines the rate at which flowers open,  $\Lambda$  is the rate of pollination of flowers,  $n$  is the number of flowers per plant, and  $\mu_p$  and  $\alpha_p$  are constant death rates for flowers and plants, respectively. Notice that constant death rates do not allow for alternate sources of death, for example fixed lifespans or flower senescence after pollination. Nevertheless, the assumption of constant death rates requires few parameters and allows for transparent interpretation of the role of death in determining phenology effects. It is also relatively general; for example,  $\alpha_p$  can be made large to approximate annuals that suffer significant losses over a single season, or small to reflect long-lived perennials with very low rates of adult mortality.

Because we are primarily interested in seed set, we include two additional state variables. The first is for pollinated dead-heads,  $D$ , by which we mean pollinated flowers that have ceased to bloom, but have not yet seeded. Dead-heads automatically become seeds unless either the plant itself is killed or else there is insufficient time to set seed before the end of the year. The

second state-variable is for flowers that have finished the seeding process,  $X$ . Ultimately, it is the value of  $X$  that will establish the opportunity for plant population growth the following year. With  $m$  being the rate of conversion from a pollinated dead head to a seeded plant, the dynamics are given by

$$\frac{dD}{dt} = \overbrace{\mu_p P}^{\text{flower death}} - \overbrace{\alpha_p n D}^{\text{plant death}} - \overbrace{m D}^{\text{seed production}} \tag{6}$$

$$\frac{dX}{dt} = \overbrace{m D}^{\text{seed production}} \tag{7}$$

Season-to-season dynamics

To quantify the cumulative effects of plant and pollinator phenologies and their interactions with changing densities, we assume the following relationship

$$U_{0,T+1} = \omega X_T(t_f) + \varrho F_{t_f,T} \tag{8}$$

where  $U_{0,T+1}$  is the total initial flower population (i.e.,  $U_0$ ) in year  $T+1$ ,  $t_f$  is the length of a single season,  $X_T(t_f)$  is the total

number of plants that have set seed in year  $T$  by time  $t_f$ ,  $F_{t_f,T} = U_T(t_f) + P_T(t_f) + D_T(t_f) + X_T(t_f)$  is the standing plant population (in terms of number of flowers) at time  $t_f$  in year  $T$ ,  $\omega$  is an amplification factor (e.g., average number of successfully germinated seeds per flower  $\times$  flowers per plant) and  $\varrho \leq 1$  is the inter-season survival of mature plants. For the sake of simplicity, we will only consider annuals from now on, with  $\varrho = 0$ .

Model parameterization and exploration

Equations (1–8) can be simplified by assuming that pollination events are fast compared to plant and pollinator demographics (Appendix A). This allows us to approximate the seven state variables in Eqs. (1–7) with a reduced system of five state variables. Because pollination events are expected to occur on the order of minutes to hours, while species demographics are expected to occur on the order of days to weeks, or even years, the approximation should be accurate for all biologically realistic scenarios. Thus, for the remainder of the paper, we will only consider the simplified model.

We will also assume that the probability density functions governing plant and pollinator phenology are gamma distributions described by

$$g_x(t, \theta_x) = \begin{cases} 0 & t \leq \varepsilon_x \\ \frac{\lambda_x}{\Gamma(\zeta_x)} (\lambda_x(t - \varepsilon_x))^{\zeta_x - 1} e^{-\lambda_x(t - \varepsilon_x)} & t > \varepsilon_x \end{cases}, \quad x = s, p \tag{9}$$

where  $\theta_x = (\lambda_x, \zeta_x)$ ,  $\lambda_x$  is the inverse scale parameter,  $\zeta_x$  is the shape parameter,  $\varepsilon_x$  is the shift, and  $\Gamma(\zeta_x)$  is the gamma function. The gamma distribution is a good choice here because it is flexible in shape, has a bounded left tail that provides a defined start point to each population’s period of activity, and is relatively parameter sparse. Gamma distributions have been used to quantify phenological variation in several previous studies (Fagan et al. 2010; Calabrese et al. 2008). One could also use other probability density functions (e.g., beta (Calabrese and Fagan 2004), logistic (Zonneveld and Metz 1991)), but typically at increased computational cost.

To characterize the phenological shift of the gamma distributions with a single number, we introduce the time points  $t_s$  and  $t_p$  that maximize  $g_s(t, \theta_s)$  and  $g_p(t, \theta_p)$ , respectively.  $t_s$  and  $t_p$  thus correspond to the times of peak pollinator arrival and peak flowering of the plant population. Likewise, we introduce  $\Delta = t_s - t_p$  as the difference in timing between the peaks of pollinator arrival and flower blooming. Note that these reference points for peak activity periods are only a convenience for illustration; the dynamics of the model retain the full range of asynchrony present for both interacting species, as advocated by Miller-Rushing et al. (2010).

We are primarily interested in changes in plant population growth rate that appear as a result of changes in plant phenology relative to that of their pollinators. To study this, we will focus on the following metric of plant population growth

$$\rho_{1000} = \left( \omega X(t_f) / U_0 \right)_{U_0=1000} \tag{10}$$

where  $U_0$  is the initial number of flowers at the start of a season and  $\omega X(t_f)$  reflects seed production at the end of the same season. Because Eq. (10) is, in essence, discrete time,  $\rho_{1000} > 1$  indicates population growth while  $\rho_{1000} < 1$  indicates population decline. Thus,  $\rho_{1000} = 1$  lies at the boundary between a viable population and a population that is predicted to go extinct. The subscript indicates that  $\rho$  is evaluated at an initial plant density of  $U_0 = 1000$ . We use this as our reference state because  $\rho = \omega X(t_f) / U_0$  exhibits a dependence on  $U_0$  for small plant populations (i.e., an Allee effect) but  $U_0 = 1000$  is sufficiently large to be beyond the influence of the Allee effect (i.e., we can estimate the limiting value of  $\rho$  for large  $U_0$ ). The Allee effect is shown in Supplemental Figure C1 for six different emergence scenarios. This Allee effect arises because

individuals that are reproducing asynchronously may become isolated in time (Calabrese and Fagan 2004). Although we do not explore this Allee effect further, we note that the initial population sizes at which it operates may be realistically small for many plant species (including tropical species, e.g., Moraes et al. (1999)).

## Results

To explore the interplay between plant phenology and plant population growth, we calculate  $\rho_{1000}$  (see Eq. 10) as a function of  $\Delta$  (the difference in timing between the peaks in pollinator arrival and flower blooming). We find that the plant population growth rate can depend sensitively on the functions defining flower opening and pollinator arrival (Eq. 9, see scenarios i–iii in Fig. 1a) and on the parameters governing the rates at which pollination-related events and demographic changes take place (see Fig. 1b–d; for examples of the full dynamics of the system, see Supplemental Figures C2–4). When the opening/arrival distributions span only a small time span, plant reproductive success falls off rapidly with changing phenology (Fig. 1b–d, scenario i). This is particularly true when flowers are short-lived and bloom before pollinators arrive, or when pollinators are short-lived and become active before flowers bloom.

Increasingly broad distributions expand the range of  $\Delta$  values over which plant population growth rates remain positive (Fig. 1b–d, scenarios ii and iii), even for short-lived flowers and pollinators. Pollinated flowers, and hence, plant population growth rates, peak at slightly negative values of  $\Delta$  (i.e., when pollinators arrive slightly ahead of plants) rather than at  $\Delta=0$  (see, for example, Fig. 1d). This asymmetry results from the finite and shaped flowering/arrival windows of the plants and pollinators, respectively. Indeed, asymmetry is not observed in the limit of infinitely narrow plant flowering and pollinator arrival peaks (see Appendix B), highlighting the need for quantitative accounting of the interplay between density and timing. Intuitively, when plants precede their pollinators, seed set and plant population growth are reduced. This effect can be extreme when either flowers are short-lived or pollinator activity is fleeting (e.g., short-lived flies or butterflies, quickly emigrating hummingbirds) (Fig. 1c, d).

We expand on these results in Fig. 2 where, for a broad range of plant and pollinator death rates (i.e., “pace of life” parameters), we identify parametric thresholds for  $\rho_{1000}=1$  (i.e., the boundary between population growth vs. population decline). This is done for a series of different plant–pollinator phenological mismatches, assuming either broad or narrow plant flowering and pollinator emergence/arrival windows. Contrasting the broad (Fig. 2a, b) and narrow windows (Fig. 2c, d), it is evident that increasing the window size expands the range of rate parameters for which the system

can tolerate a given temporal mismatch and still exhibit plant population growth (i.e.,  $\rho_{1000}>1$ ). This occurs because increased population-level asynchrony offsets decreased overlap between peak flower presence and peak pollinator presence. Ultimately, this allows for a higher frequency of successful pollination events.

In general,  $\rho_{1000}=1$  contours are non-monotonic, peaking at small values of  $\mu_p$  (Fig. 2b, d). This occurs because flowers must senesce to set seed. As a result, there is an upper limit to how long flowers can be open and have enough time to set seed before the season’s end. Increasing pollination rates ( $\Lambda$ ) permit positive plant population growth in the face of increasing plant death rates ( $\alpha_p$ ), but the benefits quickly attenuate (Supplemental Fig C5). Interestingly, the  $\Lambda$  vs.  $\alpha_p$  contours for different values of  $\Delta \leq 0$  intersect (Supplemental Fig. C5b, d). This result, which implies that some plant–pollinator interactions could persist with a slight temporal mismatch, even when an otherwise equivalent species pair with perfectly matched phenologies could not, arises because plant population growth rate peaks at small negative values of  $\Delta$  (i.e., when pollinators arrive slightly ahead of plants). This is the same asymmetry that was seen in Fig. 1d and discussed above.

## Discussion

Both individual- and population-level asynchrony contribute to the demographic consequences of phenology, and the opportunities for climate change to shape those consequences. For example, in a fig–fig wasp pollination system, within-tree asynchronous flowering increased opportunities for pollinator-mediated outcrossing and enhanced reproductive success (Gates and Nason 2012). Those empirical results support the theoretical conclusions of Post et al. (2001b) pointing to the evolutionary advantages of within-individual asynchrony as a reproductive bet-hedging mechanism in unpredictable environments. In contrast to within-individual asynchrony, population-level asynchrony emerges when individuals, which may themselves be reproducing over a window of time, develop at heterogeneous rates (e.g., Lynch et al. 2013). Our model accommodates both individual-level and population-level asynchrony, although it does not distinguish between the two. Very generally, we find that, in plant–pollinator systems, increased asynchrony enhances opportunities for successful plant reproduction (Fig. 1). This is particularly true when plants or pollinators are short-lived, in which case asynchrony can rescue a population from decline. The one caveat is that the benefit of asynchrony breaks down when plant populations are so small that Allee effects become important (Supplemental Figure C1; see also (Rathcke and Lacey 1985; Calabrese and Fagan 2004)).

In our model, we also find that season-long successful pollination is maximized when pollinator phenology slightly

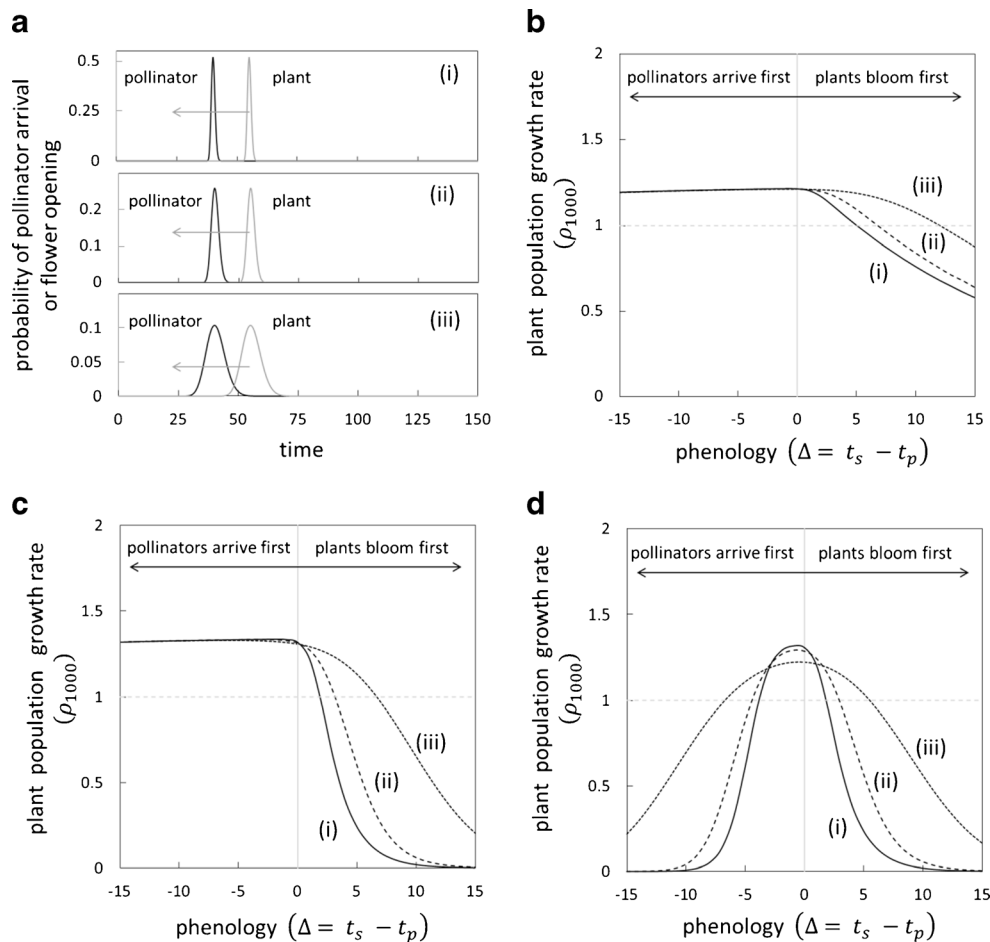


**Fig. 1** **a** The three different functions (see Eq. 9) considered for flower opening (gray) and pollinator arrival (black). The gray arrow indicates the total phenology shift associated with  $\Delta \in (-15, 15)$ , which corresponds to  $\sim 2$ -week shifts (Memmott et al. 2007). The gamma distribution parameterization is  $\zeta_s = \zeta_p = 60$  for all scenarios with (i)  $\lambda_s = \lambda_p = 10$ ,  $\varepsilon_s = 34.1$  ( $t_s = 40$ ) (ii)  $\lambda_s = \lambda_p = 5$ ,  $\varepsilon_s = 28.2$  ( $t_s = 40$ ), and (iii)  $\lambda_s = \lambda_p = 2$ ,  $\varepsilon_s = 10.5$  ( $t_s = 40$ ). **b–d** Plant population growth rates,  $\rho_{1000}$ , as a function of the separation between peak pollinator emergence and peak plant emergence for three scenarios that differ in terms of the relative rates of pollinator

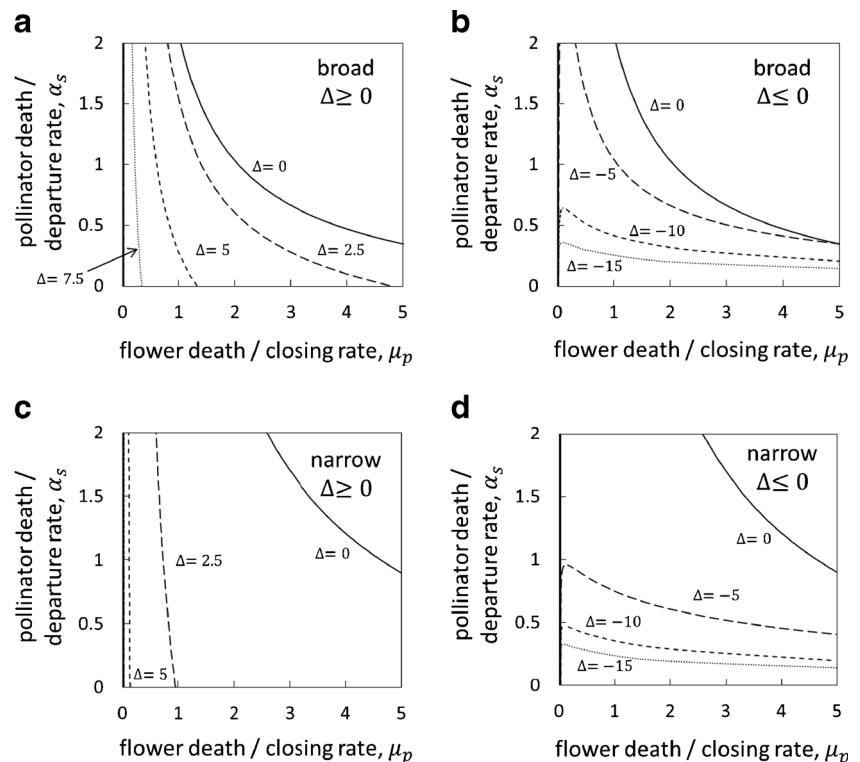
death (emigration) and flower senescence. The vertical gray line separates situations where pollinators arrive first from those where flowers appear first. The dotted horizontal gray line  $\rho_{1000} = 1$  indicates the population growth rate corresponding to a constant population size. Scenarios: **b** long-lived pollinators and long-lived flowers:  $\alpha_s = 0.075$ ,  $\mu_p = 0.05$ , **c** long-lived pollinators and short-lived flowers:  $\alpha_s = 0.075$ ,  $\mu_p = 0.5$ , and **d** short-lived pollinators and short-lived flowers:  $\alpha_s = 1$ ,  $\mu_p = 0.5$ . All other parameters are held constant as:  $\alpha_p = 0.005$ ,  $\beta = 1$ ,  $\gamma = 15$ ,  $\Lambda = 0.1$ ,  $S_0 = 1000$ ,  $t_f = 150$ ,  $m = 0.05$ ,  $\omega = 1.5$ ,  $n = 1$ , and  $\varrho = 0$

precedes flower phenology (i.e.,  $\Delta$  is slightly negative). This results from a population dynamical consequence of the interplay between the rates at which individuals enter and exit the plant and pollinator populations. A closely related dynamical phenomenon occurs in phenologically explicit two-sex models (Zonneveld 1992; Larsen et al. 2013) where, in many model scenarios, female reproductive success is maximized with a modest amount of protandry.

In addition to asynchrony and the direction of phenological mismatch, our modeling approach can also be used to explore the role of life-history parameters. This allows us to compare and contrast different kinds of plant–pollinator systems, for example orchids (long-lived flowers) versus bromeliads (short-lived flowers) (Primack 1985) or pollination by oligolectic bees (short-lived pollinators) (Schlindwein and

Wittmann 1997; Minckley 2008) versus birds (long-lived pollinators) (Rathcke 1983; Schleuning et al. 2012). In the current manuscript, we demonstrate system-level comparison by focusing on pace of life parameters, namely plant, flower, and pollinator lifespan as well as pollination rate. Specifically, we study the threshold between plant population growth and decline as a function of simultaneous changes in pairs of parameters (see Fig. 2 and Supplementary Figure C5). Certainly, any combination of pace of life parameters could be examined. Similarly, the approach could be extended to other model parameters, for instance the rate of pollen collection,  $\gamma$ , and removal,  $\beta$ , by pollinators, or overall pollinator abundance,  $S_0$ . Alternately, composite parameters could be considered. Non-dimensional parameters (see Appendix A), for example, would allow a particularly efficient exploration

**Fig. 2** Contours for the threshold separating population growth from population decay ( $\rho_{1000}=1$ ) as a function of flower death rate  $\mu_p$  and pollinator death (emigration) rate  $\alpha_s$  for broad or narrow flower opening/pollinator arrival windows and several values of  $\Delta$ . **a**  $\lambda_s=\lambda_p=2$ ,  $\varepsilon_s=10.5$  ( $t_s=40$ ); **b**  $\lambda_s=\lambda_p=2$ ,  $\varepsilon_s=10.5$  ( $t_s=40$ ); **c**  $\lambda_s=\lambda_p=5$ ,  $\varepsilon_s=28.2$  ( $t_s=40$ ); and **d**  $\lambda_s=\lambda_p=5$ ,  $\varepsilon_s=28.2$  ( $t_s=40$ ). Parameters are  $\zeta_s=\zeta_p=60$ ,  $\beta=1$ ,  $\gamma=15$ ,  $\alpha_p=0.005$ ,  $\Lambda=0.1$ ,  $S_0=1000$ ,  $t_f=150$ ,  $m=0.05$ ,  $n=1$ , and  $\omega=1.5$



of parameter space, although parameter interpretation would be problematic. Parameter choice aside, because Zonneveld models can be developed with tunable parameters governing any trait of interest, they provide a convenient method for theoretical comparison across different types of ecological systems. This enables identification of the types of systems that are likely to be most sensitive to ongoing climate change.

Outside of purely theoretical studies, Zonneveld models are advantageous because they can explicitly incorporate empirical phenology data through their rate functions (here, the functions governing pollinator arrival and flower opening in Eqs. 1 and 4, respectively). Calabrese et al. (2008) and Lynch et al. (2013) provide detailed work-ups of how such phenological linkages between data and models can be accomplished. This would be more difficult in continuous time models. Nakazawa and Doi (2012), for example, clearly illustrate a range of scenarios in which phenology could change the outcome of interspecific interactions. However, reformulating their model for any specific system would be complicated, since it lacks the flexibility and easy linkage to life-history traits that characterize Zonneveld-type models.

More generally, Zonneveld models are advantageous because they help establish a broad and flexible framework through which researchers can directly explore the demographic consequences of climatically driven phenological change, thus satisfying a key need of global change studies (Miller-Rushing et al. 2010; Post et al. 2001a). For example, at the expense of requiring additional equations, the equation system (1–7) could be expanded to investigate the dynamics

of a dioecious plant species that requires the service of a pollinator for reproduction. This would provide a way of studying systems where male and female plants have different developmental rates or are otherwise potentially divergent in their responses to climate change (Jones et al. 1999; Hedhly et al. 2009). Similarly, equation system (1–7) could be expanded to study the relative impacts of phenological changes in systems with specialist versus generalist pollinators (Memmott et al. 2007; Rafferty and Ives 2011a) (see, for example, Appendix D). Likewise, with modifications to the equation system (1–7), phenologically explicit models could be developed for other types of species interactions, such as competitive interactions, antagonistic consumer–resource interactions, or food–web modules involving multiple species (Kula 2012).

Zonneveld-type models provide one further advantage in studies of changing phenology: they can be conveniently extended to hybrid dynamical systems in which an annual cycle involves both a growing season (where phenology within and between species matters) and a non-growing season (where biological events happen, but need not be tracked in a phenologically explicit way) (Mailleret and Lemesle 2009). A hybrid dynamical system with Zonneveld dynamics for the growing season could facilitate incorporating year-to-year stochasticity in the phenology of one or both interacting species as well as in the feedback between them. This is a worthwhile avenue for investigation because increased climate variability is expected with climate change (Thompson et al. 2013) and because stochasticity appears common in

plant–pollinator systems, even to the point of changing the topology of pollination networks across years (Alarcón et al. 2008; Dupont et al. 2009). Consequently, the use of Zonneveld-type models for studying climate change may have broad application, such as in investigations of how changing phenology affects fitness (Sheriff et al. 2011).

**Acknowledgments** This research was supported by the US National Science Foundation under grants DMS-1118623 (RSC and GCC) and DMS-1225917 (WFF) and the Coordenação de Aperfeiçoamento de Pessoal de nível Superior (CAPES) grant BEX 8971/11-0 (IGV).

## References

- Alarcón R, Waser NM, Ollerton J (2008) Year-to-year variation in the topology of a plant–pollinator interaction network. *Oikos* 117(12):1796–1807. doi:10.1111/j.0030-1299.2008.16987.x
- Bascompte J, Jordano P, Melián CJ, Olesen JM (2003) The nested assembly of plant–animal mutualistic networks. *Proc Natl Acad Sci* 100(16):9383–9387. doi:10.1073/pnas.1633576100
- Both C, Bouwhuis S, Lessells CM, Visser ME (2006) Climate change and population declines in a long-distance migratory bird. *Nature* 441(7089):81–83
- Calabrese JM, Fagan WF (2004) Lost in time, lonely, and single: reproductive asynchrony and the Allee effect. *Am Nat* 164(1):25–37. doi:10.1086/421443
- Calabrese JM, Ries L, Matter SF, Debinski DM, Auckland JN, Roland J, Fagan WF (2008) Reproductive asynchrony in natural butterfly populations and its consequences for female matelessness. *J Anim Ecol* 77(4):746–756. doi:10.1111/j.1365-2656.2008.01385.x
- Doi H, Gordo O, Katano I (2008) Heterogeneous intra-annual climatic changes drive different phenological responses at two trophic levels. *Climate Res* 36(3):181
- Dupont YL, Padrón B, Olesen JM, Petanidou T (2009) Spatio-temporal variation in the structure of pollination networks. *Oikos* 118(8):1261–1269
- Edwards M, Richardson AJ (2004) Impact of climate change on marine pelagic phenology and trophic mismatch. *Nature* 430(7002):881–884
- Encinas-Viso F, Revilla TA, Etienne RS (2012) Phenology drives mutualistic network structure and diversity. *Ecol Lett* 15(3):198–208. doi:10.1111/j.1461-0248.2011.01726.x
- Fagan WF, Cosner C, Larsen EA, Calabrese JM (2010) Reproductive asynchrony in spatial population models: how mating behavior can modulate Allee effects arising from isolation in both space and time. *Am Nat* 175(3):362–373
- Forrest J, Inouye DW, Thomson JD (2010) Flowering phenology in subalpine meadows: does climate variation influence community co-flowering patterns? *Ecology* 91(2):431–440. doi:10.1890/09-0099.1
- Forrest JRK, Thomson JD (2011) An examination of synchrony between insect emergence and flowering in Rocky Mountain meadows. *Ecol Monogr* 81(3):469–491. doi:10.1890/10-1885.1
- Gates DJ, Nason JD (2012) Flowering asynchrony and mating system effects on reproductive assurance and mutualism persistence in fragmented fig–fig wasp populations. *Am J Bot* 99(4):757–768. doi:10.3732/ajb.1100472
- Gilman RT, Fabina NS, Abbott KC, Rafferty NE (2012) Evolution of plant–pollinator mutualisms in response to climate change. *Evol Appl* 5(1):2–16. doi:10.1111/j.1752-4571.2011.00202.x
- Harder LD, Johnson SD (2005) Adaptive plasticity of floral display size in animal-pollinated plants. *Proc R Soc B Biol Sci* 272(1581):2651–2657
- Hedhly A, Hormaza JI, Herrero M (2009) Global warming and sexual plant reproduction. *Trends Plant Sci* 14(1):30–36. doi:10.1016/j.tplants.2008.11.001
- Hill JK, Hodkinson ID (1995) Effects of temperature on phenological synchrony and altitudinal distribution of jumping plant lice (Hemiptera: Psylloidea) on dwarf willow (*Salix lapponum*) in Norway. *Ecol Entomol* 20(3):237–244. doi:10.1111/j.1365-2311.1995.tb00453.x
- Iler AM, Inouye DW (2013) Increasing temporal synchrony between syrphid flies and their floral resources despite differential phenological responses to climate change. *Global Change Biology*. In press
- Inouye DW (2008) Effects of climate change on phenology, frost damage, and floral abundance of montane wildflowers. *Ecology* 89(2):353–362. doi:10.1890/06-2128.1
- Johansson J, Smallegange IM, Jonzén N (2012) An eco-evolutionary model for demographic and phenological responses in migratory birds. *Biology* 1(3):639–657
- Jones MH, MacDonald SE, Henry GHR (1999) Sex- and habitat-specific responses of a high arctic willow, *Salix arctica*, to experimental climate change. *Oikos* 87(1):129–138. doi:10.2307/3547004
- Kula AR (2012) Quantifying context-dependent outcomes of the interaction between *Silene stellata* (Caryophyllaceae) and its pollinating seed predator, *Hadena ectypa* (Noctuidae), a potential mutualist.
- Larsen E, Calabrese JM, Rhoads M, Fagan WF (2013) How protandry and protogyny affect female mating failure: a spatial population model. *Entomologia Experimentalis et Applicata* 146(1):130–140. doi:10.1111/eea.12003
- Lynch HJ, Rhoads M, Calabrese JM, Cantrell S, Cosner C, Fagan WF (2013) How climate extremes—not means—define a species’ geographic range boundary via a demographic tipping point. *Ecological Monographs*
- Maillet V, Lemesle V (2009) A note on semi-discrete modelling in the life sciences. *Philos Trans R Soc A Math Phys Eng Sci* 367(1908):4779–4799
- McKinney AM, CaraDonna PJ, Inouye DW, Barr B, Bertelsen CD, Waser NM (2012) Asynchronous changes in phenology of migrating broad-tailed hummingbirds and their early-season nectar resources. *Ecology* 93(9):1987–1993
- Memmott J, Craze PG, Waser NM, Price MV (2007) Global warming and the disruption of plant–pollinator interactions. *Ecol Lett* 10(8):710–717. doi:10.1111/j.1461-0248.2007.01061.x
- Miller-Rushing AJ, Høye TT, Inouye DW, Post E (2010) The effects of phenological mismatches on demography. *Philos Trans Royal Soc B: Biol Sci* 365(1555):3177–3186. doi:10.1098/rstb.2010.0148
- Minckley R (2008) Faunal composition and species richness differences of bees (Hymenoptera: Apiformes) from two north American regions. *Apidologie* 39(1):176–188
- Moraes PLRD, Monteiro R, Vencovsky R (1999) Conservação genética de populações de *Cryptocarya moschata* Nees (Lauraceae) na Mata Atlântica do estado de São Paulo. *Revista brasileira de Botânica* 22(Suppl 2):237–248
- Nakazawa T, Doi H (2012) A perspective on match/mismatch of phenology in community contexts. *Oikos* 121(4):489–495. doi:10.1111/j.1600-0706.2011.20171.x
- Parnesan C (2007) Influences of species, latitudes and methodologies on estimates of phenological response to global warming. *Glob Chang Biol* 13(9):1860–1872. doi:10.1111/j.1365-2486.2007.01404.x
- Post E, Forchhammer MC, Stenseth NC, Callaghan TV (2001a) The timing of life—history events in a changing climate. *Proc R Soc Lond Ser B Biol Sci* 268(1462):15–23
- Post E, Levin SA, Iwasa Y, Stenseth NC (2001b) Reproductive asynchrony increases with environmental disturbance. *Evolution* 55(4):830–834



- Primack RB (1985) Longevity of individual flowers. *Annu Rev Ecol Syst* 16:15–37. doi:10.2307/2097041
- Rafferty NE, Ives AR (2011a) Effects of experimental shifts in flowering phenology on plant–pollinator interactions. *Ecol Lett* 14(1):69–74. doi:10.1111/j.1461-0248.2010.01557.x
- Rafferty NE, Ives AR (2011b) Pollinator effectiveness varies with experimental shifts in flowering time. *Ecology* 93(4):803–814. doi:10.1890/11-0967.1
- Rathcke B (1983) Competition and facilitation among plants for pollination. *Pollination biology*: 305–329
- Rathcke B, Lacey EP (1985) Phenological patterns of terrestrial plants. *Annu Rev Ecol Syst* 16:179–214. doi:10.2307/2097047
- Rodriguez J, Jordano D, Haeger JF (1994) Spatial heterogeneity in a butterfly–host plant interaction. *Journal of Animal Ecology*:31–38
- Rudolf VH, Singh M (2013) Disentangling climate change effects on species interactions: effects of temperature, phenological shifts, and body size. *Oecologia*:1–10
- Russell FL, Louda S (2004) Phenological synchrony affects interaction strength of an exotic weevil with Platte thistle, a native host plant. *Oecologia* 139(4):525–534. doi:10.1007/s00442-004-1543-1
- Schleuning M, Fründ J, Klein A-M, Abrahamczyk S, Alarcón R, Albrecht M, Andersson GK, Bazarian S, Böhning-Gaese K, Bommarco R (2012) Specialization of mutualistic interaction networks decreases toward tropical latitudes. *Current Biology*
- Schlindwein C, Wittmann D (1997) Stamen movements in flowers of *Opuntia* (Cactaceae) favour oligolectic pollinators. *PI Syst Evol* 204(3–4):179–193. doi:10.1007/bf00989204
- Schwartz MD, Hanes JM (2010) Intercomparing multiple measures of the onset of spring in eastern North America. *Int J Climatol* 30(11):1614–1626. doi:10.1002/joc.2008
- Sheriff MJ, Kenagy GJ, Richter M, Lee T, Tøien Ø, Kohl F, Buck CL, Barnes BM (2011) Phenological variation in annual timing of hibernation and breeding in nearby populations of Arctic ground squirrels. *Proc R Soc B Biol Sci* 278(1716):2369–2375. doi:10.1098/rspb.2010.2482
- Sherry RA, Zhou X, Gu S, Arnone JA, Schimel DS, Verburg PS, Wallace LL, Luo Y (2007) Divergence of reproductive phenology under climate warming. *Proc Natl Acad Sci* 104(1):198–202. doi:10.1073/pnas.0605642104
- Thompson RM, Beardall J, Beringer J, Grace M, Sardina P (2013) Means and extremes: building variability into community-level climate change experiments. *Ecol Lett* 16(6):799–806. doi:10.1111/ele.12095
- Visser ME, Both C (2005) Shifts in phenology due to global climate change: the need for a yardstick. *Proc R Soc B Biol Sci* 272(1581):2561–2569. doi:10.1098/rspb.2005.3356
- Visser ME, Holleman LJM (2001) Warmer springs disrupt the synchrony of oak and winter moth phenology. *Proc R Soc Lond Ser B Biol Sci* 268(1464):289–294. doi:10.1098/rspb.2000.1363
- Visser ME, Noordwijk AJV, Tinbergen JM, Lessells CM (1998) Warmer springs lead to mistimed reproduction in great tits (*Parus major*). *Proc R Soc Lond Ser B Biol Sci* 265(1408):1867–1870. doi:10.1098/rspb.1998.0514
- Zipkin EF, Ries L, Reeves R, Regetz J, Oberhauser KS (2012) Tracking climate impacts on the migratory monarch butterfly. *Glob Chang Biol* 18(10):3039–3049. doi:10.1111/j.1365-2486.2012.02751.x
- Zonneveld C (1992) Polyandry and protandry in butterflies. *Bull Math Biol* 54(6):957–976
- Zonneveld C, Metz J (1991) Models on butterfly protandry: virgin females are at risk to die. *Theoret Pop Biol* 40(3):308–321